

## Numerical Simulation of RC Beams Reinforced with Internal Steel Trusses

Salah El-Din F. Taher<sup>1</sup>, Hamdy M. Afefy<sup>2</sup>, Omnia F. Khroub<sup>3</sup>, Sally Salem<sup>4</sup>

<sup>1</sup>Professor of Concrete Structures, Structural Engineering Dept., Faculty of Engineering, Tanta University, Egypt

E-mail: [salah.taher@f-eng.tanta.edu.eg](mailto:salah.taher@f-eng.tanta.edu.eg)

<sup>2</sup>Professor of Concrete Structures and Head of Construction Engineering and Management Department, Pharos University in Alexandria, Egypt. On leave from Tanta University  
E-mail: [hamdy.afefy@pua.edu.eg](mailto:hamdy.afefy@pua.edu.eg) and [hamdy.afefy@f-eng.tanta.edu.eg](mailto:hamdy.afefy@f-eng.tanta.edu.eg)

<sup>3</sup>Professor of Steel Structures, Structural Engineering Dept., Faculty of Engineering, Tanta University, Egypt

E-mail: [omnia\\_m102010@f-eng.tanta.edu.eg](mailto:omnia_m102010@f-eng.tanta.edu.eg)

<sup>4</sup>Master Student at Structural Engineering Dept., Faculty of Engineering, Tanta University, Egypt

E-mail: [egsallyaly@gmail.com](mailto:egsallyaly@gmail.com)

### ABSTRACT

This paper presents numerical investigation on the overall structural behavior of reinforced concrete beams provided with different configurations of embedded steel trusses as web reinforcement. Five specimens having the same dimensions as well as the longitudinal reinforcement were modeled using ABAQUS software. One beam was reinforced with traditional vertical web reinforcement, while the remaining beams were provided with different truss' layout. The main studied criteria were the ultimate failure load, the cracking load, the cracking pattern, principle tensile strain vectors on stirrups and the load versus the mid-span deflection curve. The numerical results showed that using embedded steel truss as web reinforcement resulted in increased the ultimate capacity of the beam by range of (4%-8%) compared to that of the control beam reinforced with traditional vertical stirrups.

**Keywords:** ABAQUS software, Embedded Steel Truss, Finite Element Modeling, Reinforced Concrete Beams, Flexural.

### 1. Introduction

Over years, several steel configurations have been developed and used as an alternative to the traditional vertical steel stirrups for shear resisting such as steel trusses embedded in the girders, steel panels as shear reinforcements, and thin walls to form a composite section. This section combined the advantage of concrete and steel where concrete is better in compression and steel is better in tension so that the section has high strength, stiffness, and durability.

Arafa et al. [1] investigated the shear performance, failure load, and mid-span deflection of reinforced concrete beam having embedded steel trusses with different shear span to depth ratios ranged between 1 and 2.5. Their test results showed that all beams provided with embedded steel truss failed by flexural mode in spite that the corresponding control beams failed in shear. Prahallada et al. [2] studied the behavior of conventional steel-reinforced concrete beam which replaced by pre-fabricated (lattice-warren) steel truss as reinforcement. The results showed that the beam provided with steel trusses exhibited higher flexural and shear capacities. Alias and Vijayan [3] studied the effect of hybrid materials on strengthening of deep beams. It was found that the shear strength of the beam reinforced by hybrid steel trussed showed higher shear strength compared to that reinforced with conventional steel.

Djamaluddin et al. [4] showed that the flexural capacity of RC beam reinforced by truss system reinforcement had been increased by about 13%.

Ammash [5] studied experimentally and numerically the behavior of RC beams provided with steel strip plates having different thickness as shear reinforcement instead of conventional stirrups. The result showed the efficiency of the steel strips in controlling the crack width as well as increasing the ultimate capacity noticeably. Also, Ballarini et al. [6] investigated numerically the failure behavior of hybrid steel trussed concrete beam (HSTCB) having different sizes of specimen under three point bending loading. Yas et al. [7] studied numerically the effect of using different arrangements of the steel truss in order to improve the confinement stresses in both shear and flexural regions. The results showed that the ultimate load increased by either using truss arrangement or by providing inclined stirrups. In the sequel, Dinesh and Anuragi [8] conducted numerical study on the effect of various truss configurations on the shear and flexure behavior. The results showed the enhanced behavior owing to the improved confinement stress. Zhang et al. [9] studied experimentally and theoretically the shear performance of reinforced concrete beams provided with embedded steel trusses. The results showed that the reinforced concrete beams reinforced with embedded steel truss had better shear performance compared with common reinforced concrete beams where the ultimate shear strength was increased by 80%. Saju and Usha [10] studied the flexural behavior of reinforced concrete beams reinforced with two types of truss arrangements. The results showed that the failure of the beams with vertical stirrups was sudden compared to that of beam with truss reinforcement. Besides, the beams reinforced with truss reinforcements were less deflected during the service load stage, and had more strength and stiffness than those of the corresponding beams reinforced with vertical reinforcement. Dhanush and Rao [11] studied the effect of angle of inclination, size and the depth of embedment of truss connector on the load carrying behavior of RC beams. The results showed that the load capacity increased as the angle of inclination of the truss connectors increased up to  $60^\circ$ .

In the current paper, different configurations of the internal steel trusses were provided along the entire span of the beams. And then the effect of their configurations on the controlling failure criteria was investigated numerically using ABAQUS software.

## 2. Verification of Simulation Results

In this part, the accuracy of ABAQUS software in simulation of RC beams is verified. Two phases were considered where experimental test results of selected beams were compared with the results of the program simulation.

### 2.1 Phase One of Verification

The experimental results of three simply supported beams tested by [2] were selected to be compared with the numerical results. The first beam reinforced with conventional vertical stirrups, while the second and the third beams reinforced with pre-fabricated steel trusses. The geometric properties as well as the reinforcement configurations are shown in Figs. (1) to (3).

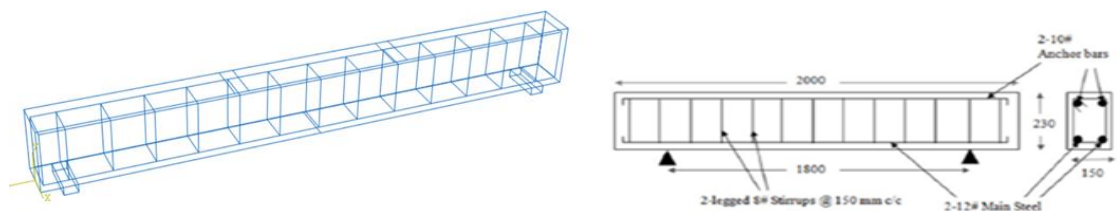


Fig. 1 Reinforcement detailing of conventionally reinforced RC beam B1 [2].

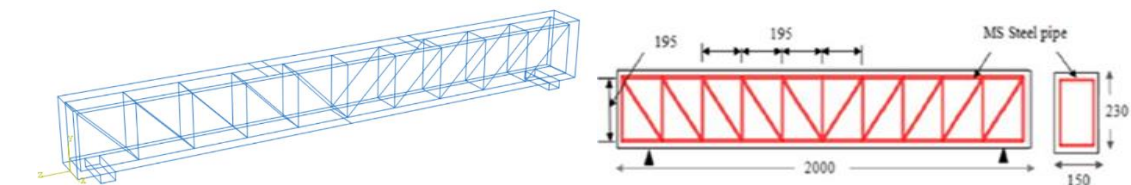


Fig. 2 Reinforcement detailing of conventionally reinforced RC beam B2 [2].

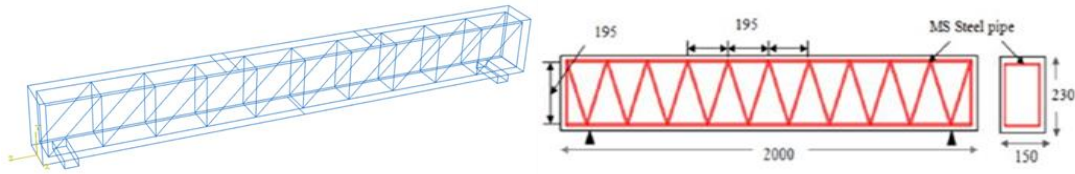


Fig. 3 Reinforcement detailing of conventionally reinforced RC beam B3 [2].

### 2.1.1 Material Properties

The material properties for both concrete and reinforcing steel are described herein below. The material properties of the used concrete at the elastic range are the Young's modulus and the Poisson's ratio, where were 22360 MPa and 0.2, respectively. For inelastic behavior of concrete, the concrete damage plasticity model (CDP) was adopted to model concrete behavior. CDP allows for separate yield strengths, strain rates, and damage parameters in tension and compression. It assumes that the main two failure mechanisms are tensile cracking and compressive crushing of the concrete material.

For the compressive stress-strain curve of the concrete, the stress-strain relationship proposed by Park and Paulay [12] as illustrated by Eqs. (1) and (2) was used to construct the uniaxial compressive stress-strain curve for concrete as shown in Fig. 4(a).

$$\text{when } \varepsilon \leq 0.002, \quad f_c = f_c' \left[ 2 \frac{\varepsilon_c}{\varepsilon_0} - \left( \frac{\varepsilon_c}{\varepsilon_0} \right)^2 \right] \quad (1)$$

$$\text{when } 0.002 \leq \varepsilon \leq 0.0035, \quad f_c = f_c' \left[ 1 - 0.15 \frac{\varepsilon - \varepsilon_0}{\varepsilon_{cu} - \varepsilon_0} \right] \quad (2)$$

Under uniaxial tension, the stress-strain response follows a linear elastic relationship until the value of the failure stress,  $\sigma_{10}$ , is reached; the failure stress corresponds to the onset of micro-cracking in the concrete material. Beyond the failure stress the formation of micro-cracks is represented macroscopically with a softening stress-strain response, which induces strain localization in the concrete structure. Under uniaxial compression the response is linear until the value of initial yield,  $\sigma_{c0}$ . In the plastic regime, the response is typically characterized by stress hardening followed by strain softening beyond the ultimate stress,  $\sigma_{cu}$ . As for stress-strain relationship under uni-axial tension up to ultimate tensile strength, the elastic parameters are elastic modulus,  $E_c$ , and tensile strength,  $f_{ct}$  that can be calculated by ACI equations as follows [13]:

$$E_c = 4700 \sqrt{f_{cy}} \quad (\text{MPa}) \quad (3)$$

$$f_{ct} = 0.33 \sqrt{f_{cy}} \quad (\text{MPa}) \quad (4)$$

Where  $f_{cy}$  is the cylinder compressive strength.

In the current study, stress-displacement method was used to estimate the post peak stress-deformation relationship of concrete under uni-axial tension load as represented in Fig. 4(b). The fracture energy  $G_f$  can be calculated by the following equation proposed by Hillerborg et al. [14].

$$G_f = 110 \frac{f_{cy}^{0.18}}{10} \quad \text{Jole/m}^2 \quad (5)$$

The behavior of reinforcing steel bars was assumed to be bilinear elasto-plastic material and identical in tension and compression. Elastic behavior of steel material is defined by specifying Young's modulus ( $E_s$ ) and Poisson's ratio ( $\nu$ ) of typical values of  $2 \times 10^5$  MPa and 0.3, respectively. The plastic young modulus is assumed to be  $0.1E_s$ . The bond between steel



**Table 2 comparisons of finite element and an experimental ultimate load of reinforced beam**

| Beam | $P_{UEXP}$ kN | $P_{UFE}$ kN | $P_{UFE}/P_{UEXP}$ |
|------|---------------|--------------|--------------------|
| B1   | 55.96         | 62.04        | 1.11               |
| B2   | 62.85         | 63.86        | 1.02               |
| B3   | 60.42         | 60.20        | 0.99               |

**2.2 Second Phase of Verification**

In this phase, two beams tested by [4] were chosen. The first beam reinforced with conventional steel (BN), while the second beam reinforced with welded steel truss (BR). The geometric properties and the configuration of the used steel are shown in Fig. 6 and Fig. 7.

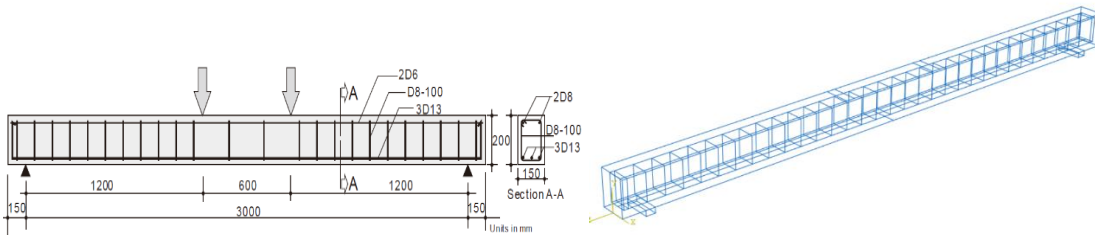


**Fig. 6 Details of BN type beam [4].**

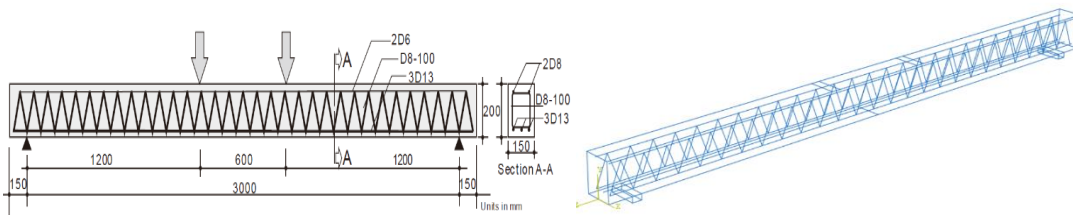


**Fig. 7 Details of BR type beam [4].**

Fig. 8 shows comparison between the experimental and the numerical load-deflection curves for both beams. It can be observed that the numerical simulation could capture well the experimental behavior where the variation of the numerical ultimate load was no more than 3% the corresponding experimental load.

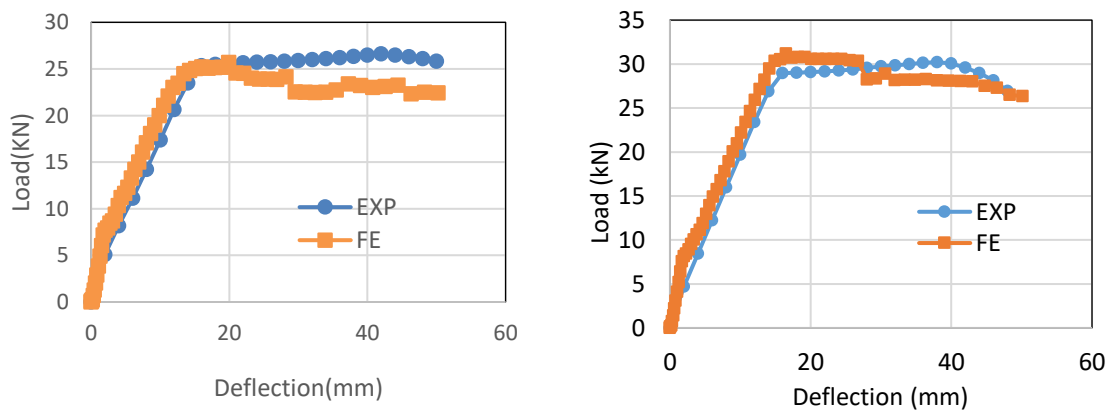


**Fig. 8 Comparison between experiment and numerical load-deflection curves.**

**3. Objectives and Methodology of the Current Research**

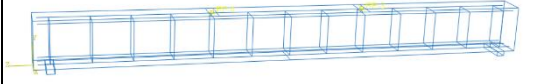
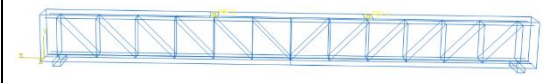
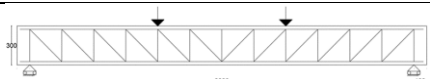
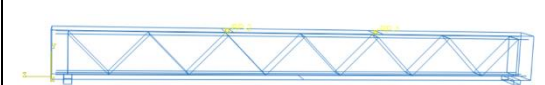
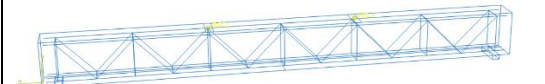
In the current research, different configurations of internal steel trusses are studied as an alternative to traditional steel reinforcement in reinforced concrete beams. The main objectives of the study are to investigate the following criteria

- 1- The maximum ultimate load of the beam for different truss shapes.
- 2- Failure shapes for different trussed beams.
- 3- Growth of cracks under (25% - 50% - 75% - 95%) of the maximum ultimate load.
- 4- Assign which stirrup has maximum strain.
- 5- Determine the maximum strain vectors for (reinforcing steel and stirrups) under the maximum ultimate load.

**4. Structural Model and Material Properties**

In this paper, five reinforced concrete beams (B0-B1-B2-B3-B4) have been modeled using ABAQUS software to figure out the best shape of internal steel truss to resist the acting load. All of them has same materials and geometry, cross-section of 200x300 mm and total length of 3200 mm. The lower longitudinal steel was 3Ø12mm, while the upper steel was 2Ø8mm. Smooth mild steel was used for stirrups of 8 mm diameter. The concrete compressive strength was 25MPa, while the yield stress for all reinforcement was 240MPa. The Poisson's ratio for concrete and steel are 0.2 and 0.3, respectively. All beams were loaded by four points loading system. B0 consider as control beam where it is provided with conventional vertical stirrups. The remaining beams (B1-B2-B3-B4) were provided with different configuration for trussed-stirrups as shown in Table 3.

**Table 3 Reinforcement configurations versus numerical simulation for internal steel reinforcement**

| Beam       | ABAQUS simulation   | Reinforcement configuration  |
|------------|---|--|
| B0 control |  |  |
| B1         |  |  |
| B2         |  |  |
| B3         |  |  |
| B4         |  |  |

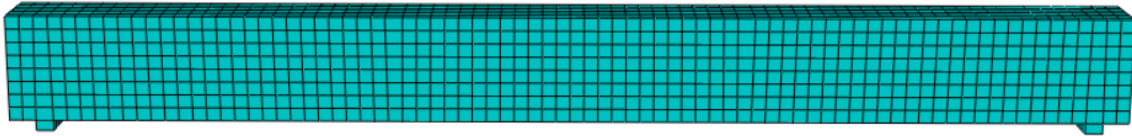
The concrete damaged plasticity model (CDP) is used to simulate the concrete behavior. Table 4 summarizes the recommendation value of (CDP) under compound stress. The behavior of concrete under uniaxial compression and tension was modeled as illustrated formerly. The steel material was defined as bilinear elasto-plastic stress-strain curve with linear strain hardening as illustrated in the verification clause.

**Table 4 the used values of (CDP) parameters**

| Parameter name                                     | Value |
|--|-------|
| Dilation angle                                     | 36    |
| Flow potential eccentricity                        | 0.1   |
| Biaxial/uniaxial compression plastic strain ration | 1.16  |
| Invariant stress ration                            | 0.67  |
| Viscosity  | 0     |

#### 4.1 Finite Element Mesh

8-node three-dimensional linear brick, reduced integration, hourglass control element, namely C3D8R, was used for representing concrete. The solid 8-node element (C3D8R) activates the three translational degrees of freedom at each nodes  $u$ ,  $v$ , and  $w$  in  $x$ ,  $y$ , and  $z$  directions. On the other hand, A 2-node linear three-dimensional truss element namely T3D2 was used for steel embedded in concrete tension and compression zones as well as the internal trusses. There are three translational degrees of freedom at each of nodes of (T3D2) truss elements  $u$ ,  $v$ ,  $w$  in  $x$ ,  $y$ , and  $z$  directions. The mesh model of concrete is presented in Fig. 9.

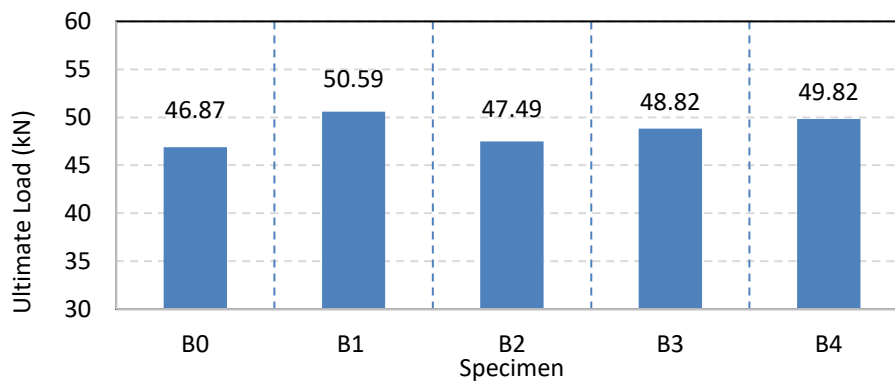
**Fig. 9 Concrete mesh.**

## 5. Results and Discussions

The results include ultimate failure load of the beam, cracking load, load-deflection curve at mid-span, growing of cracks, maximum strain vectors for (longitudinal steel- stirrups), and assign which stirrups has maximum strain.

### 5.1 Ultimate Failure Load of Beams

Beams with truss arrangement as reinforcement gave better flexural strength than that of control beam reinforced with conventional vertical stirrups, where the strut effect of the inclined bars increase the flexural strength. It was found that B1 has maximum ultimate load with about 8% increases compared with conventional beam B0. Fig. 10 shows comparison among the ultimate loads for all beams.

**Fig. 10 Ultimate loads for all beams.**

**5.2 Load-deflection curves**

Fig. 11 shows the load-deflection curves for all beams up to failure for the mid-span section. The curves of all beam were almost linear pattern up to yield value and after that plastic behaviors were controlled the behavior. With further loading, the developed cracks on the concrete tensile zone were spread as well as the internal longitudinal and transversal steel reinforcement yielded. Thus, failure of all beams was developed characterized by ductile manner as shown in Fig. 11. It can be observed that the beam B1 provided with N-truss stirrups exhibited the outermost performance among all beams.

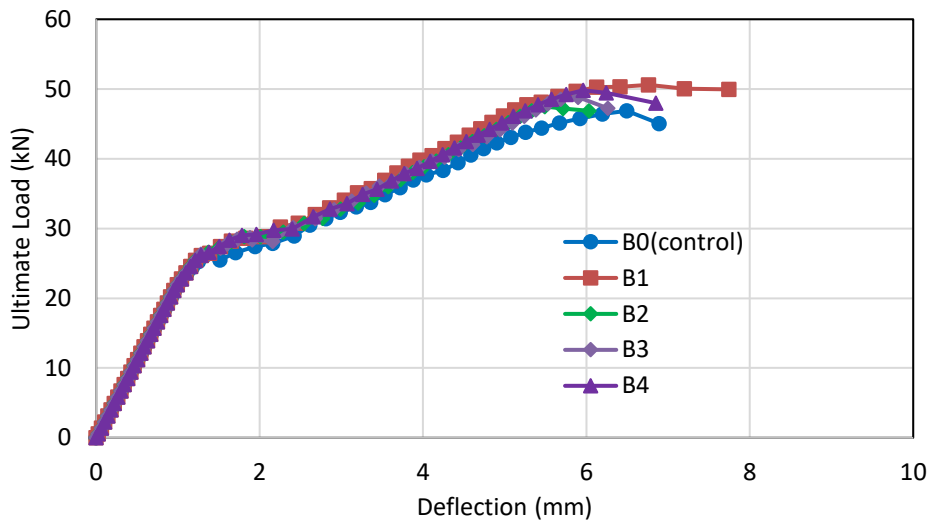


**Fig. 11 Load deflection curves for all beams.**

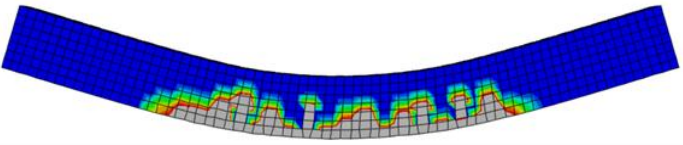
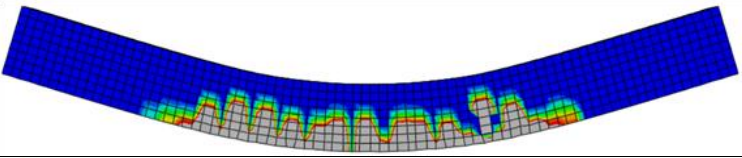
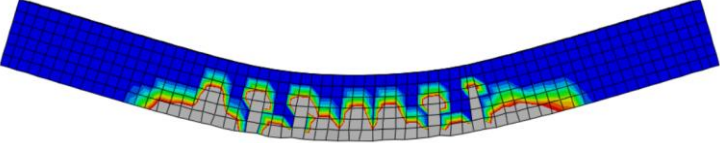
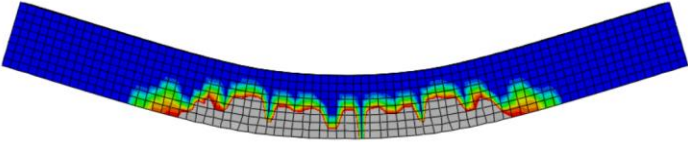
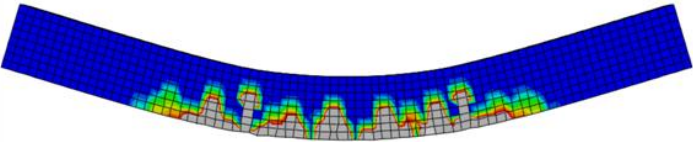
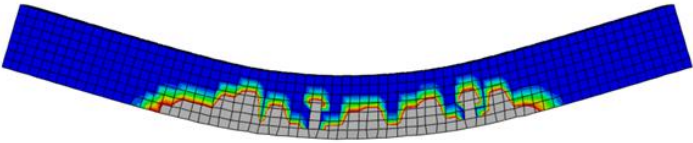
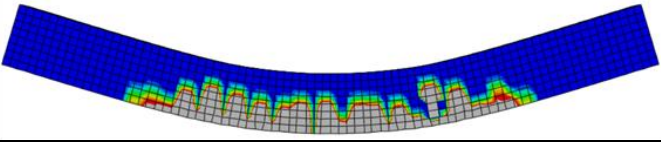
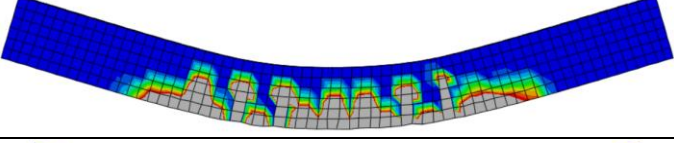
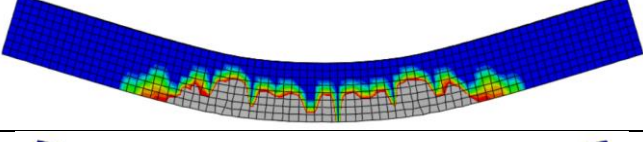
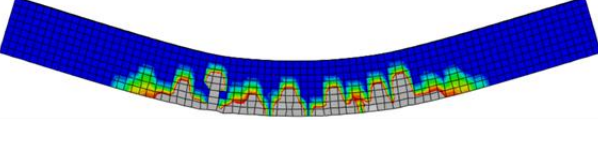
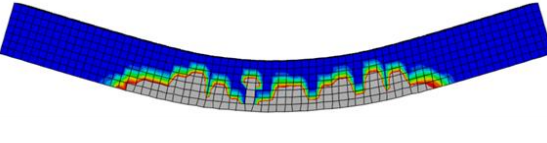
**5.3 Crack Pattern**

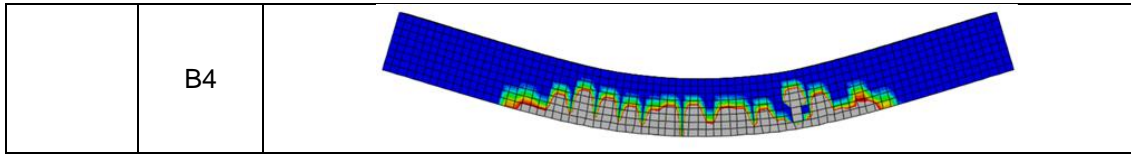
All beams are failed in flexural, where the tensile stresses of the concrete were exhausted and exceed the specified tensile strength of concrete. In general, first flexural cracks occurred approximately at the same vertical load at mid span section. And then when applied load increased, vertical flexural cracks extended horizontally and cover long region from tensile side of the beam. The propagation of cracks was monitored at different stages of loading as a percentage of the beam's ultimate load (25%-50%-75%-95%-100%) as depicted in Table 5.

**Table 5 Propagation of tensile cracks for all beams at different stages of loading**

| % from $P_u$ | Beam       | Growing cracks |
|--------------|------------|----------------|
| 25% $P_u$    | B0 control |                |
|              | B1         |                |

|       |            |  |
|-------|------------|--|
|       | B2         |  |
|       | B3         |  |
|       | B4         |  |
| 50%Pu | B0 control |  |
|       | B1         |  |
|       | B2         |  |
|       | B3         |  |
|       | B4         |  |
| 75%Pu | B0 control |  |
|       | B1         |  |
|       | B2         |  |

|        |            |  |
|--------|------------|--|
|        | B3         |    |
|        | B4         |    |
| 95%Pu  | B0 control |    |
|        | B1         |    |
|        | B2         |   |
|        | B3         |  |
|        | B4         |  |
| 100%Pu | B0 control |  |
|        | B1         |  |
|        | B2         |  |
|        | B3         |  |



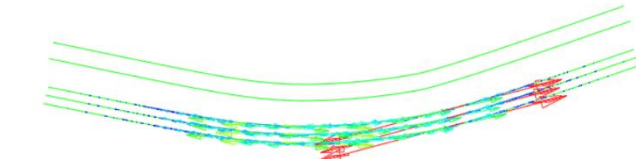
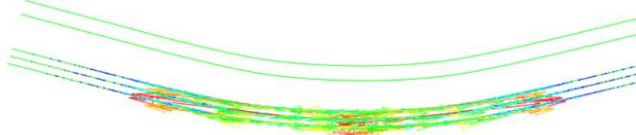
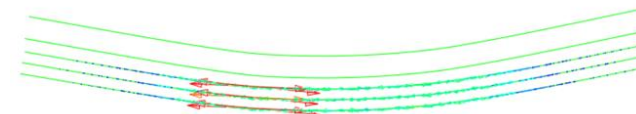
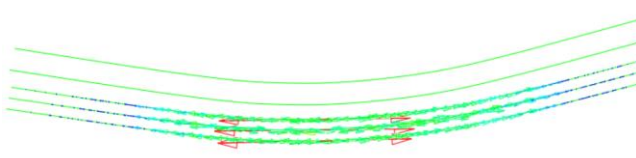
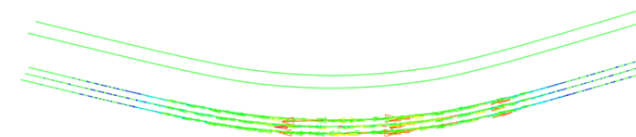
**5.4 Steel behavior**

In this section, the behavior of lower longitudinal steel bars is illustrated as shown in table 6. As the acting load increased, the lower steel for all beams elongated, deformed, and reached the yield stress. Tables 6 and 7 show the principle strain vectors for longitudinal steel which indicated the highest position of tensile stress in the lower steel where it was different from beam to another under effect of the same load. After the longitudinal steel bars reached the yielding point, the stirrups were affected on the load. Table 8 shows the strain vectors for stirrups which indicate to which stirrups has the maximum strain due to load. From results the maximum strain for stirrups appear in the middle of the beam near to the load effect.

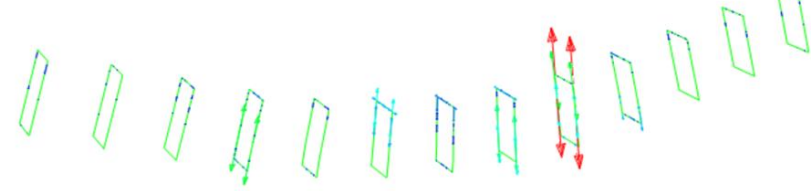
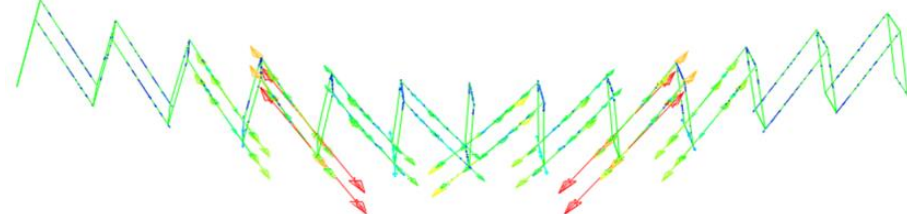
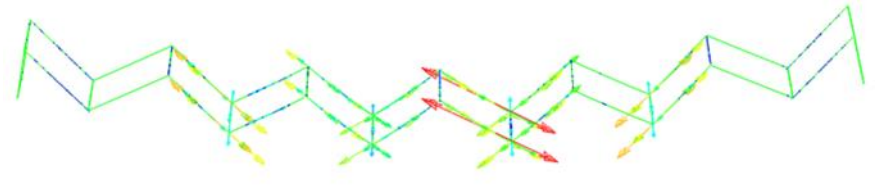
**Table 6 Steel von Mises stresses**

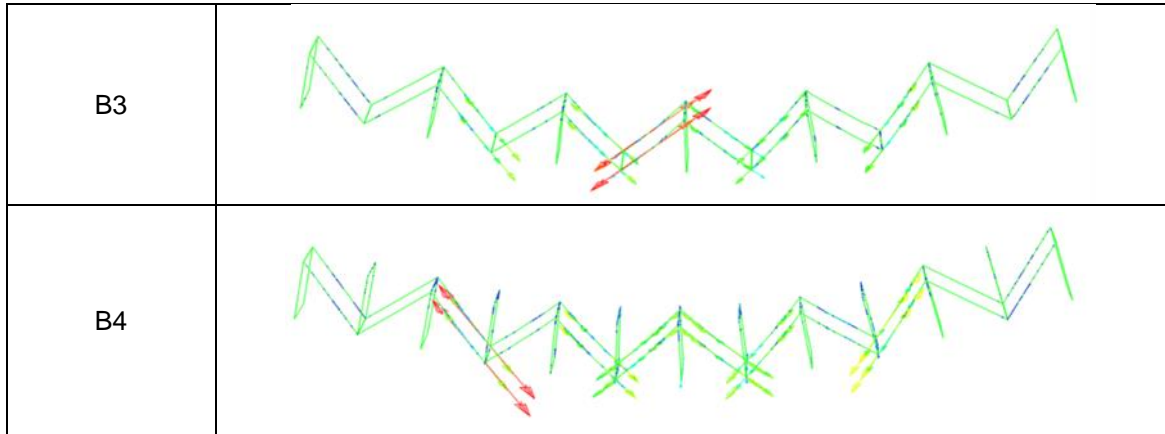
| Beam         | Steel von Mises |
|--------------|-----------------|
| B0 (control) |                 |
| B1           |                 |
| B2           |                 |
| B3           |                 |
| B4           |                 |

**Table 7 Strain vectors for longitudinal steel**

| Beam        | Strain vectors for steel  |
|-------------|---|
| B0(control) |   |
| B1          |   |
| B2          |   |
| B3          |   |
| B4          |  |

**Table 8 Strain vectors for internal stirrups**

| Beam        | Strain vectors for stirrups  |
|-------------|--|
| B0(control) |  |
| B1          |  |
| B2          |  |



### 5.5 Finite element results

Table 9 summarizes the finite element results which indicate that, the first crack for all beams were the same, where the first cracks depended on concrete material. In general, embedded truss increase the ultimate load due to effect of inclined members in truss that develop some resistance. B1 has maximum ultimate load which showed about 8% increases compared with that of the conventional beam B0, but the weight of the used steel was the highest one compared to others. On the other hand, B2 increased the ultimate load by about 1% compared with B0, however, it has the minimum weight of steel truss.

**Table 9 Finite element results**

| Beam         | $P_u$ (kN) | Ratio $P_u/P_{ucontrol}$ | Deflection At $P_u$ (mm) | $P_{cr}$ (kN) | $P_y$ (kN) | Truss Weight (Kg) | Specific U.L | Ratio Specific U.L |
|--------------|------------|--------------------------|--------------------------|---------------|------------|-------------------|--------------|--------------------|
| B0 (control) | 46.87      | 1.00                     | 6.49                     | 22            | 30         | 14988.10          | 0.003        | 1.00               |
| B1           | 50.59      | 1.08                     | 6.75                     | 22            | 30         | 19761.75          | 0.0026       | 0.87               |
| B2           | 47.49      | 1.01                     | 5.48                     | 22            | 30         | 16285.75          | 0.0029       | 0.97               |
| B3           | 48.82      | 1.04                     | 5.90                     | 22            | 30         | 17865.75          | 0.0027       | 0.90               |
| B4           | 49.82      | 1.06                     | 5.96                     | 22            | 30         | 19761.75          | 0.0025       | 0.83               |

### 6. Conclusion

Based on the results of the finite element simulation of embedded trussed beam for five different configurations taking into account the used material properties and reinforcement configurations, the following conclusions can be drawn: -

- All beams were failed by flexural mode failure.
- All beams reinforced with embedded steel trusses gave higher ultimate flexural strength compared to that of control beam reinforced with traditional vertical stirrups. The increases of the ultimate load reached up to 8% when N-truss was used as beam B1.
- For all beam, the stirrups which had the maximum tensile strain was located in the mid-span region adjacent to the acting load.

**REFERENCES**

- 1- Arafa, M., Alqedra, M., Salim, R., (2018), "Performance of RC Beams with Embedded Steel Trusses Using Nonlinear FEM Analysis," " *Advances in Civil Engineering*," Vol.8, PP.1-8.
- 2- C. P., T., N., Y., C., (2018), " Behavior of Pre-Fabricated Steel Truss as Reinforcement in RC Beams," " *International Journal of Pure and Applied Mathematics*," Vol. 120, No.6, PP. 6691-6708.
- 3- Alias, C., and Vijayan, V., (2018), " Analytical Study on the Behavior of Hybrid Steel Trussed Concrete Deep Beam" *International Journal of Innovative Science, Engineering & Technology*," Vol. 5, No. 4, PP.132-136.
- 4- Djamaluddin, R., Frans, P., and Irmawati, R., (2017), " Flexural Capacity of the Concrete Beams Reinforced by Steel Truss System" , " *Matec Web of Conferences*" , 138,02003.
- 5- K., Haider, (2017), " Behavior of Reinforcement Concrete Beams Using Steel Strips as a Shear Reinforcements", Vol.12, No.19, PP. 8681-8688.
- 6- Ballarini, R., Mendola, L., Le, J., ASCE, A., and Monaco, A., (2017), " Computational Study of Failure of Hybrid Steel Trussed Concrete Beams", *Journal of Structural of Engineering*", Vol.143, No.8, PP.1-13.
- 7- Yas V, N., K, M., and P, P., (2017), "Analysis of Hybrid Steel Trussed Concrete Beam Using ANSYS", *International Journal of Innovative Research in Science, Engineering and Technology*, Vol. 6, No. 4, PP. 6876-6883.
- 8- Dinesh, D., and P., A., (2017), "Numerical Study of Hybrid Steel Trussed Concrete Beam", *International Research Journal of Engineering and Technology*, Vol. 4, No. 5, PP.1564-1568.
- 9- Zhang, N., FU, C. C., Chen, L., and He, L. (2016), " Experimental Studies of Reinforced Concrete Beams Using Embedded Steel Trusses", *ACI Structural Journal*, Vol.113, No. 4, PP. 701-710.
- 10- Saju, S., and Usha, S. (2016), "Study on Flexural Strength of Truss Reinforced Concrete Beams", *International Research Journal of Engineering and Technology*, Vol. 3, No. 7, PP.1541-1545.
- 11- Dhanush, S., and Rao, K., (2015), "Study of Behavior of Composite Beams with Truss Type Shear Connector", *International Journal of Research in Engineering and Technology*, Vol. 4, No. 3, PP. 289295.
- 12- Park, R and Paulay, T. *Reinforced Concrete Structures*. John Wiley & Sons, Inc., 2009.
- 13- ACI Committee 318, 2019. *Building Code Requirements for Structural Concrete (ACI 318-19) and Commentary (ACI 318R-19)*. American Concrete Institute, Farmington Hills, MI, 2019.
- 14- Hillerborg, M. M, and P. P. (1976) *Analysis of crack formation and crack growth in concrete by means of fracture mechanics and finite elements*. *Journal of Cement and Concrete Research*, Vol. 6, No. 6, PP. 73-87.